Modelling of Folding Patterns in Flat Membranes and Cylinders by Origami*

Taketoshi NOJIMA**

This paper describes folding methods of thin flat sheets as well as cylindrical shells by modelling folding patterns through Japanese traditional Origami technique. New folding patterns have been devised in thin flat squared or circular membrane by modifying so called Miura-Ori in Japan (one node with 4 folding lines). Some folding patterns in cylindrical shells have newly been developed including spiral configurations. Devised foldable cylindrical shells were made by using polymer sheets, and it has been assured that they can be folded quite well. The devised models will make it possible to construct foldable/deployable space structures as well as to manufacture foldable industrial products and living goods, e.g., bottles for soft drinks.

Key Words: Adaptive Structures, Modelling, Design, Space Equipment, Foldable Structures, Deployment

1. Introduction

Aeronautical and space structures are required to be rigid and ultralight. Moreover, because space structures are constructed in space by deploying compactly stowed ones, they must be designed so that they can be effectively deployed; developments of compact and effective stowing/deploying techniques will decide the success of the constructions of space structures[1]. These folding/deploying techniques will be diverted to devise new industrial products and living goods which are foldable, and also to design such new ultralight structural components as core materials.

Fundamental designs of foldable structures have been often investigated by using origami models. Miura[2),(3)] has proposed an origami pattern of squared membranes easily deployable. This folding pattern has been applied to simulate a unfolding of tree leaves by Kobayashi et al.[4]. Applications of origami technique to engineering field as well as theoretical treatments are very few; only in Fusimi's work[5], Guest and Pellegrino's works[6] and Miura's work mentioned above.

The purpose of this paper is to present some basic models of foldable products made of thin membranes by using origami techniques. These kinds of models will make it possible to invent not only space structures but also to produce facilely foldable such containers as, e.g., PET bottles for soft drinks. They can be kept compactly folded and also be disposable in a neatly folded condition. In this paper, after investigating geometrical conditions to design foldable cylinders, and producing some models by a polymer sheet, their folding properties are studied.

2. Folding Method

2.1 Fundamental relations

Consider a conventional origami folding by straight lines. Intersecting point of some fold lines is named node (see Fig. 1), where point 0 is a node. Mountain fold (MF) and valley fold (VF) lines are drawn by solid and dotted lines, respectively. It has been reported that when a paper sample is perfectly folded, the number of fold lines to form a node is given by Eq. (1);

$$|N_m - N_v| = 2 \tag{1}$$

where N_m and N_v are the numbers of MF and VF lines. Put the total number of fold lines N_t. Because of $N_m + N_v = N_t$, $N_t = 2(1+N_v)$; the N_t is even. Minimum number of fold lines to fold perfectly at a node is 4. The fold method using 4 fold lines is named 1-4

* Received 21st December, 2000. Japanese original: Trans. Jpn. Soc. Mech. Eng., Vol. 66, No. 643, C (2000), pp. 1050-1056 (Received 19th July, 1999)

** Graduate School of Kyoto University, Department of Aeronautics and Astronautics, Yoshida Honmachi, Sakyo-ku, Kyoto 606-8501, Japan. E-mail: nojima@impact.kuaero.kyoto-u.ac.jp

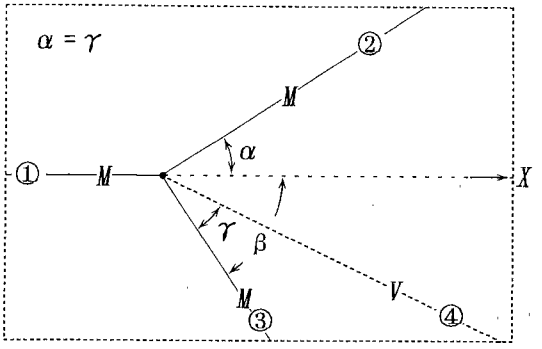

Fig. 1 Angle relation between fold lines to form one node (1 node with 4 folding lines; named 1-4 folding) (solid line; mountain fold, dotted line; valley fold)

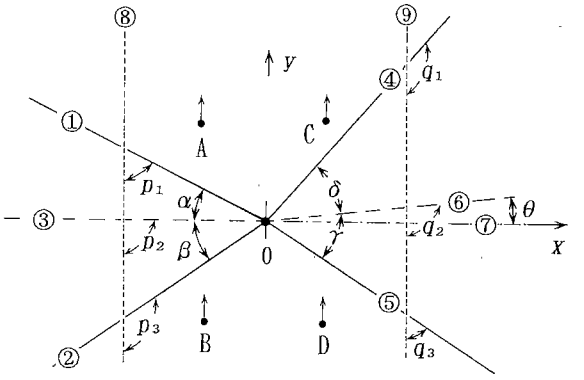

Fig. 2 Typical fold pattern for 1-6 folding and its perfectly folding condition

folding and the method with 6 fold lines is named 1-6 folding in this paper.

2.2 Folding condition

By fixing MF line ① on X axis in Fig. 1, and by introducing other MF lines ② and ③, a paper sample is folded by producing a VF line ④. By denoting forming angles of ② with X axis, and ③ with X axis by α and β, and also the angle of ③ with ④ by γ, the perfectly folding condition is given by

$$\gamma=\alpha \qquad (2)$$

When $\alpha=\beta$, the X axis is not bent in Y axis direction, but the axis of right part of the node turns backwards by angle 2α.

Next, folding condition of 1-6 folding is formulated (Fig. 2), where 2 VF lines (③, ⑥) are situated between 4 MF lines (①, ②, ④, ⑤). Line ③ is the producion of the line ①. Forming angles of ① with ③, and ② with ③ are denoted by α and β, respectively. Forming angles of ④ with ⑥, and ⑤ with ⑥ are δ and γ, respectively. Angle of ⑥ with ⑦ is denoted by θ. X-Y axis is denoted as shown in the figure (0; the node). Draw a line ⑧ orthogonal to X axis. Forming angles of lines ①, ③ and ② with ⑧ are denoted by p_1, p_2 and p_3, respectively. Forming angles of ④, ⑥ and ⑤ with another orthogonal line to X axis (⑨) are denoted by q_1, q_2 and q_3, respectively. The angles $p_1 \sim p_3$ and $q_1 \sim q_3$ are expressed by $p_1=\pi/2-\alpha$, $p_2=\pi/2$, $p_3=\pi/2+\beta$, and $q_1=\pi/2+\delta+\theta$, $q_2=\pi/2+\theta$, $q_3=\pi/2-\gamma+\theta$, respectively. By folding at MF lines ①, ② and VF line ③, two vectors (drawn at points A, B) in $X<0$ region form the angle of $-\alpha+\beta+\pi/2\ (\equiv P_L)$. By folding at MF lines ④, ⑤ and VF line ⑥, two other vectors (drawn at points C, D, $X>0$) form the angle of $\delta-\gamma+\theta+\pi/2\ (\equiv Q_R)$. Because the points A and C and also the points B and D are on the same planes, respectively, $P_L=Q_R$ holds when a sample is folded perfectly at this node. This relation is expressed by

$$\beta-\alpha=\delta-\gamma+\theta \qquad (3)$$

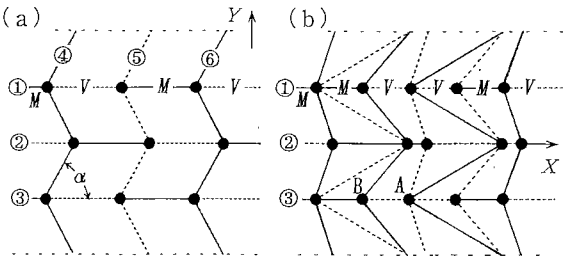

Fig. 3 (a) Miura Ori (folding) (1-4 folding), (b) An example to fold plane paper to another plane state (combination of 1-4 and 1-6 foldings)

It is easily seen that by combining alternate mountain and valley folds in 1-4 folding, strip papers become a jigzag state. On the other hand, they become cylindrical by only mountain or by only valley folds. The former is called "plane fold", and the latter is called "cylindrical fold" in this report.

3. Plane Foldings

3.1 Plane foldings by 1-4 folding

Figure 3(a) shows the simplest model for plane folding called Miura ori in Japan. It has been reported that the model is used to design solar battery arrays for space structure. This model consists of 3 horizontal fold lines (①-③) and 3 zigzag MF, VF and MF lines (④-⑥). Horizontal lines ①-③ are alternately MF⇄VF lines, and fold lines ④-⑥ are symmetrical for horizontal ones satisfying Eq.(1). As a result, folding condition, Eq.(2), holds for any value of α. Then a sheet sample is perfectly folded in direction, shrinking in direction (shrinking amount depends on α value). This fold method makes it possible to fold a squared sample from $Y=-\infty$ to $+\infty$, because the mountain and valley folds appear alternately at both sides of each node.

3.2 Plane folds by 1-6 folding

By combining symmetrical 1-4 and 1-6 fold

methods, zigzag type plane folds are possible. An example of fold pattern and its folded appearance are shown in Fig. 3(b) and 4(b), respectively. In this 1-6 folding, because fold mode (MF/VF) in X direction does not change in both sides of a node, 1-6 folding results in a formation of cylindrical shells. Then to perform zigzag type plane folds, 1-4 folding must be combined with 1-6 folding.

3.3 Generalization of 1-4 folding method

Even when the horizontal fold lines are periodically zigzaged (Fig. 5(a)), the fold condition, Eq. (2), is also satisfied; another plane fold is possible. When a flat sheet is incompletely folded, the sheet becomes a corrugated state; a thin sheet can be converted to a rigider core structure. An example of such a core made of polypropylene sheet is shown in Fig. 5(b).

When the zigzag lines in Fig. 5(a) are successively bent in the same direction, circular or sector shaped membrane can be folded in radial direction. Figure 6 shows an example of such model consisting of 6 pieces of equiangular triangles (vertical angle; 2Θ), where circumferential folding lines change their direction by 2Θ. Alternately drawn MF and VF lines in radial direction ⑦, ⑧$\cdots$ are zigzag within an angle Θ, and they form an angle α_0 at points A~C on the edge. Because the foldig lines are periodical, the angle β in the figure is $\alpha+\Theta$. By denoting forming angle of circumferential fold line ① with radial fold line by $\alpha_1 = \alpha - \Theta$, Eq.(2) is satisfied; by choosing $\alpha_1 = \alpha_0 - \Theta$, $\alpha_2 = \alpha_0 - 2\Theta$, $\cdots$ successively, folding conditions hold at all nodes. By these procedures, fold patterns of foldable circular/sector shaped membranes can be designed.

As shown in Fig. 7, even when horizontal folding lines (①-⑥) are not parallel, foldable pattern of Miura type can be obtained by drawing fold lines (⑦, ⑧) symmetrically and equiangularly to ①-⑥ at all nodes. In the pattern, initial angles (α_1, β_1) can be chosen arbitrarily. Appearance for folded sample of Fig. 7(a) is shown in Fig. 7(b). Figure 8 shows a special model whose horizontal fold lines are inclined at $\pm\Theta$ periodically. Folded samples of Figs. 6 and 8 are shown in Fig. 9(a) and (b), respectively.

4. Cylindrical Folding

By the fundamental considerations described above, it is easily seen that foldable cylinders can be devised by using successive mountain folding. Some models of such foldable cylinders are designed in the

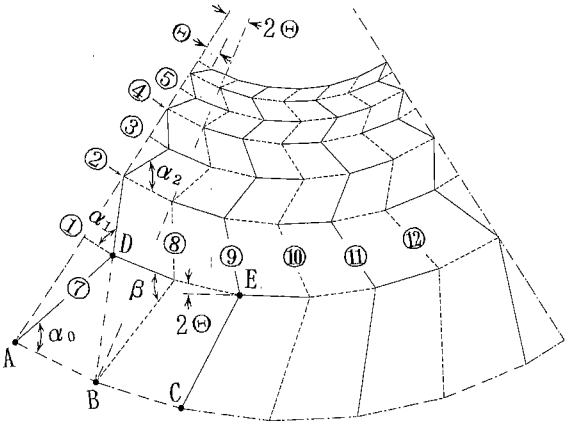

Fig. 6 A new folding pattern for circular plate

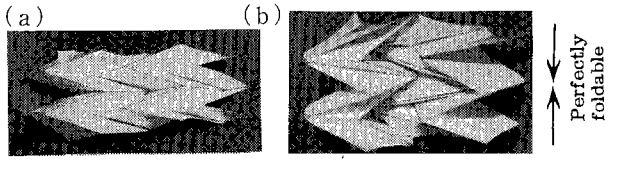

Fig. 4 Appearances of folded samples ((a) and (b) correspond to the fold patterns in Figs. 3(a) and (b))

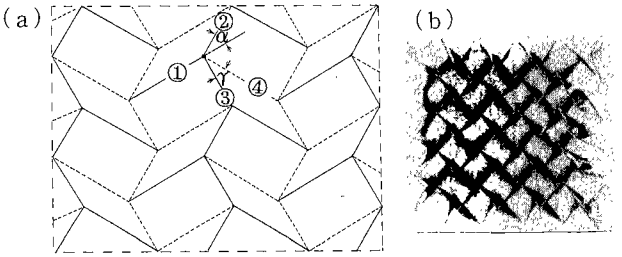

Fig. 5 Zig/zag type 1-4 folding (a), imperfectly folded polypropylene sheet to form a rigider plate (b)

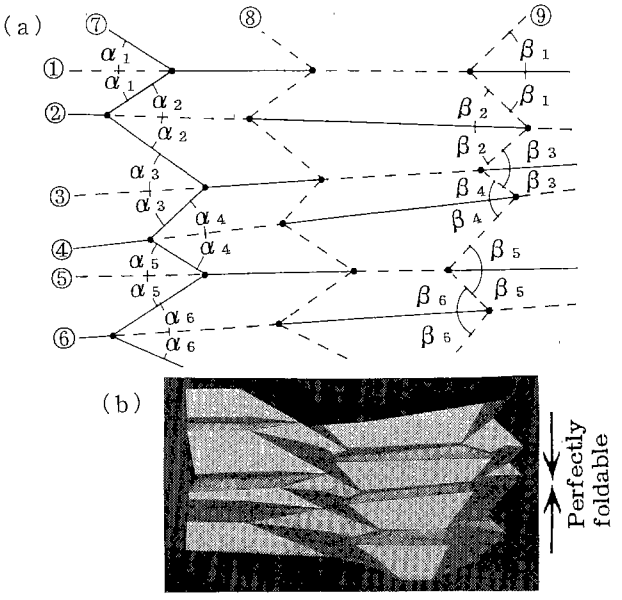

Fig. 7 A model of generalized Miura-Ori (a), and corresponding folded sample (b)

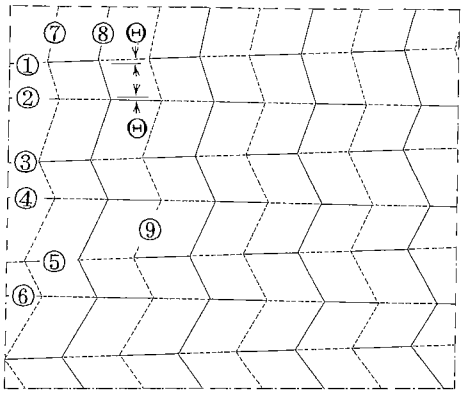

Fig. 8 An example of generalized Miura-Ori folding

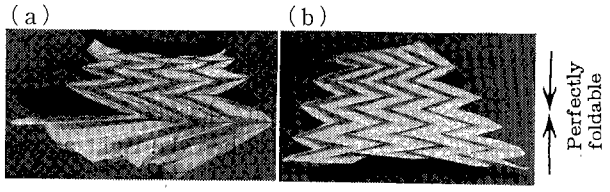

Fig. 9 (a) and (b) Photos of folded paper samples corresponding to the patterns of Fig. 6 and Fig. 8

following sections.

4.1 Origami model of a strip paper

Consider foldings of a strip which has N-fold lines (N; even) consisting of alternate MF and VF lines or successive MF lines (Fig. 10(a)). Put forming angles of fold lines with X axis by $\theta_1, \theta_2, \theta_3, \cdots$. The directions of X axis after folding are $X_1, X_2, \cdots$. By the first folding operation at ①, the right side part of the strip is turned over, and X direction of the part bends to X_1. Its bent angle is $2\theta_1$ (Fig.10(b)). By the second operation at ②, new X-axis bends to X_2. Then total bent angle is $2\theta_1-2\theta_2$.

By the 3rd operation, the bent angle of the axis becomes $2\theta_1-2\theta_2+2\theta_3$. By these operations, front and back surfaces appear alternately, and after N times folding operations, the X_N axis and the X axis form an angle of Θ_N. The Θ_N is expressed by

$$\Theta_N=2\{\theta_1-\theta_2+\theta_3 \cdots \theta_N\} \qquad (4)$$

To design foldable cylinders, two opposite edges of the strip must be glued after folding; $\Theta_N=2\pi$ must hold. This relation is called "closing condition in circumferential direction".

4.2 Cylindrical folding by using horizontal major folding lines

By regarding the upper and the lower edges of the strip as horizontal fold lines and by aligning some strips in direction, developments of foldable cylinders are designed. Examples of such developments consisting of 1-4 and 1-6 foldings patterns are shown in Fig. 11(a) - (g). Horizontal lines are named major fold

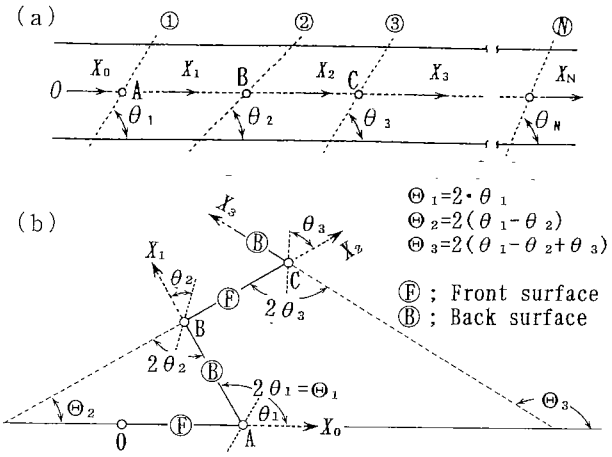

Fig. 10 Fold lines in a strip (a), and the changes of strip directions through the folding operation

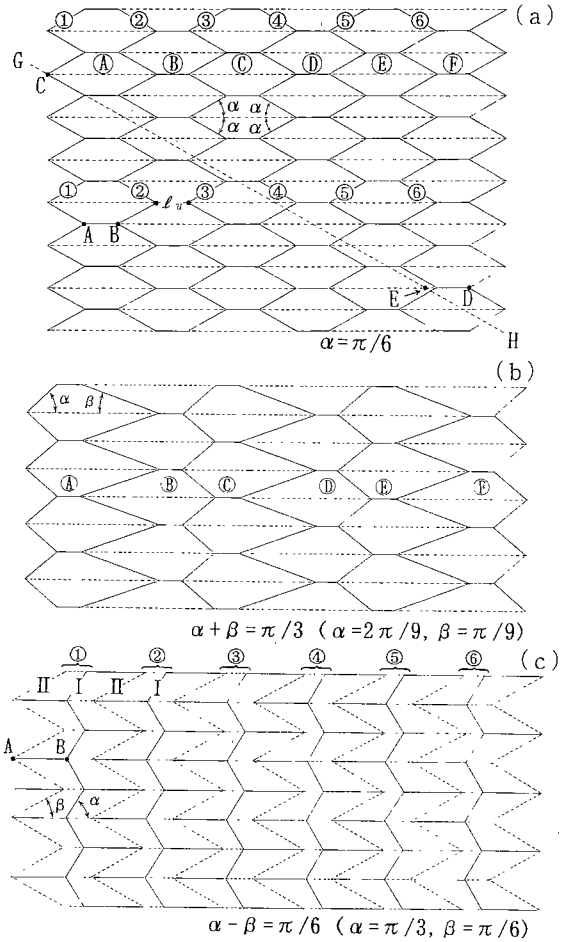

Fig. 11 (a) - (c) Representative development to form foldable cylinder (major fold lines; horizontal)

lines. As is well known, when a narrow strip is equidistantly folded N times by the angle $(N-2)/N\cdot\pi$, it forms N sided regular polygons after folding. A representative development by 1-4 folding patterns is shown in Fig. 11(a), where even numbered folding lines are oppositely directed to get fold pattern with only mountain folds ($N=6$). All fold lines form the

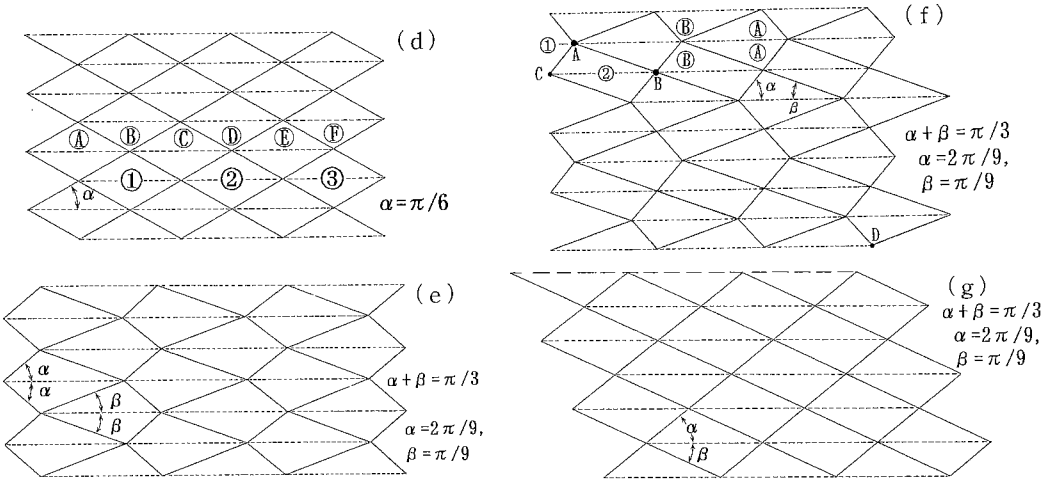

Fig. 11 (d) - (g) (continued) Developments to form foldable cylinders (major fold lines; horizontal)

angle $\alpha=\pi/6$ with the horizontal fold lines ($2\alpha=\pi/3$). Figure 11(b) consists of scalene trapezoid elements with base angles α and β ($\alpha+\beta=\pi/3$). Another pattern consisting of trapezoid elements is shown in Fig. 11(c). This pattern is obtained by replacing 6 MF lines of fold angle $\pi/3$ in Fig. 11(a) by 6 pairs of MF (I) and VF (II) lines, where α and β are arbitrary as far as $\alpha-\beta=\pi/6$.

By putting the segment $\overline{AB}=0$ in Fig. 11(a), Fig. 11(d) is derived. The pattern consists of 3 diamonds in horizontal direction, giving typical plastic buckling model of cylindrical shells. By the same way, Fig. 11(e) is obtained from Fig. 11(b).

Although 5 models above consist of symmetrical fold lines to horizontal ones, different 2 types of folding patterns can be drawn by using symmetrical pattern by every other step. Typical example is shown in Fig. 11(f). In the figure, folding condition (Eq.(3)) holds at point A because of its symmetry. Equation (3) also holds at point B. By using the folding pattern at point B in Fig. 11(f), another development can be derived (Fig. 11(g); $\alpha+\beta=\pi/3$, $\alpha=7\pi/36$, $\beta=5\pi/36$).

4.3 Foldable cylinders by using inclined major folding lines (spiral configuration)

By inclining the horizontal major fold lines, developments of Fig. 11(a) - (f) can be reformed to spiral configurations; Fig. 12(a) is obtained from Fig. 11(d) by inclining $\pi/6$ to holizontal lines. 3 diamonds ① - ③ in the figure correspond to the ones in Fig. 11(d). It is easily seen that this figure is equivalent to Fig. 12(b). The continuity of the pattern is satisfied when opposite edges of the development are glued to form a cylinder. Models shown in Fig. 12(c) - (e) are obtained from Fig. 11(a) - (c) by inclining the patterns by $\pi/6$; e.g., Fig. 12(c) is obtained by cutting the line CH in Fig. 11(a) and taking it as the base line.

Figures 12(d) and (e) are derived from Fig. 11(b) and (c), respectively. When the right and the left edges are glued, the developments of these patterns are not generally continuous. Details of the continuity condition of the patterns will be explained later. Figure 12(f) is derived from Fig. 11(f) by cutting line AD of Fig. 11(f) and putting it as a base line. The angle of about 0.193π is the forming angle of line AD with holizontal line.

By numerical simulations, Guest et al. studied possibilities to form foldable cylinders of spiral configurations where major fold lines spiral up by one or two steps every time they make a round. An example of such development is drawn in Fig. 12(g), where the right end of line ① is continuous to the left end of line ④. Though they analyzed possibility of foldability/extensibility by numerical simulations, they did not refer to perfectly foldable condition. Newly devised simpler model shown in Fig. 12(h) is proposed in this report. Foldable condition of this model does not depend on the angle β. Figure 12(i) is the repeating type of spiral configurations reformed from Fig. 12(h). This pattern can be also derived by coinciding points A and B in Fig. 11(c).

4.4 Continuity of fold patterns for spiral configurations

As is mentioned above, the fold patterns for spiral mode are not necessarily continuous when opposite edges of a development are glued to form a cylinder. For developments consisting of trapezoid elements, the continuity is realized by choosing adequate length of l_u in Fig. 11(a). The length can be determined as follows (Fig. 13); by taking 0 as an origin, and drawing N pieces of trapezoids on inclined major fold line direction (the angle φ), point A is settled. Denoting the height of the trapezoids by h, the length $\overline{OA}$ is

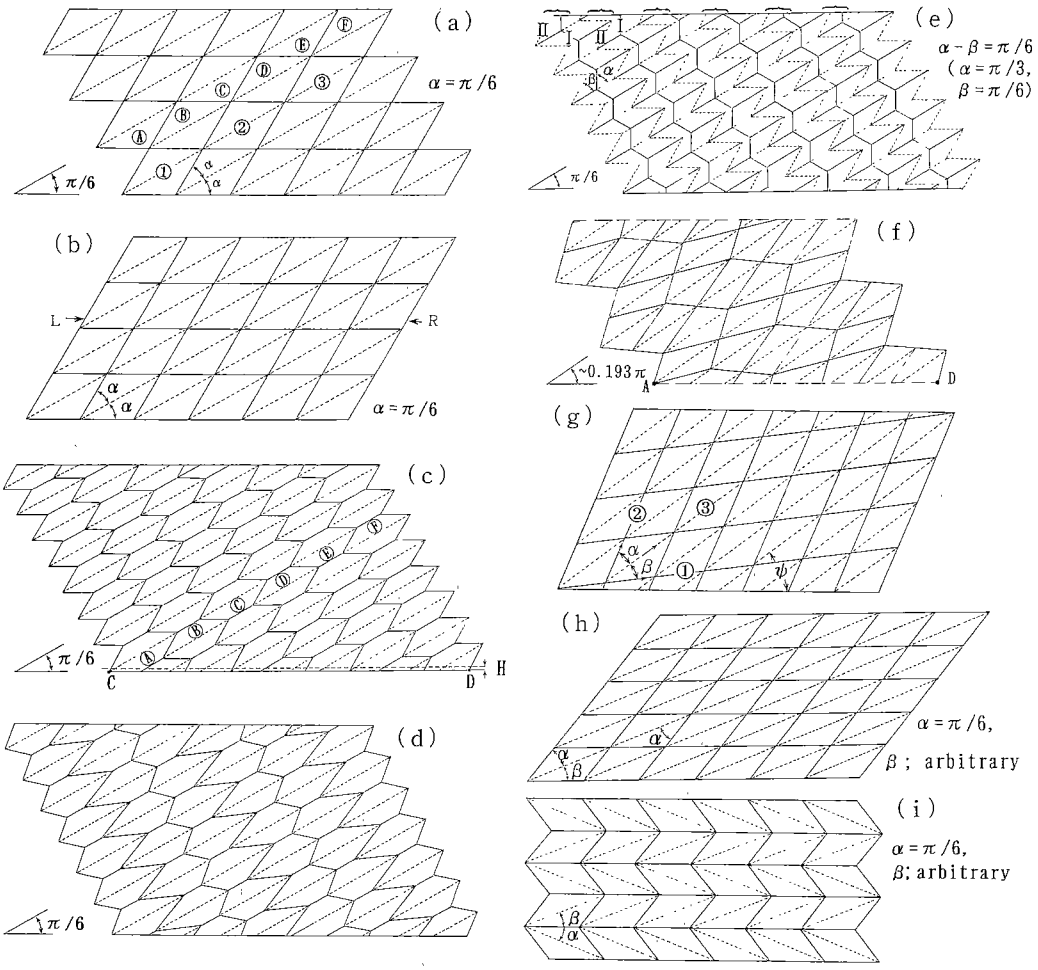

Fig. 12 Developments to form foldable cylinders (major fold lines; inclined) giving spiral models

given by $N(h+\tan\theta+l_u)$. By drawing m (m; even) pieces of the same shaped trapezoids under N-th trapezoid, point B is determined as shown in the figure. For the continuity of patterns, point B should be on X axis. Because the length AB is mh, the l_u is given by

$$l_u=(2N-m\tan\varphi/\tan\theta)h/\tan\varphi \qquad (5)$$

By using the l_u value, continuous patterns can be derived.

4.5 Verification of circumferential closing condition

By using two representative examples, circumferential closing condition ($\Theta_N=2\pi$) will be studied below. For Fig. 12(c), the condition is checked for a narrow band near the base line (band width; H). In the band, there are 18 fold lines consisting of 3 groups with 6 fold lines. Using $\varphi=\pi/6$, the rotation angle of the Θ axis given by Eq.(4) becomes

$$\Theta_N=2\{(\alpha+\varphi)-\varphi+\varphi-\varphi+(\alpha+\varphi)-\varphi\}\times3=12\alpha \qquad (6)$$

By putting $\alpha=\pi/6$, Eq.(6) is 2π; the closing condition is satisfied. For Fig. 12(h), it is checked by using 6 parallelograms along X axis. The rotating angle

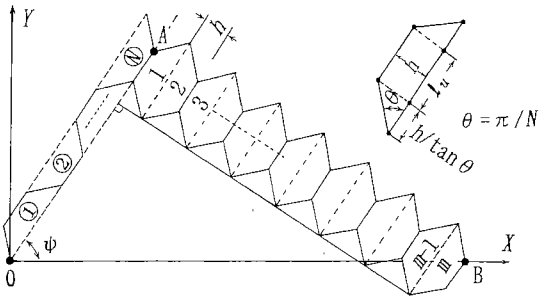

Fig. 13 Schematic description to determine l_u length to obtain continuous development in Figs. 12(c), (d) and (e)

becomes

$$\Theta_N=2\{(\alpha+\beta)-\beta\}\times6=12\alpha \qquad (7)$$

Putting $\alpha=\pi/6$, the condition ($\Theta_N=2\pi$) is also satisfied. It is noted by Eq.(7) that the condition is independent of β value. For the model presented by Guest et al. (Fig. 12(g)), this closing condition becomes $(N+1)\alpha-\beta=\pi$; $\alpha=\beta=\pi/6$ will be a representative model.

Except for Fig.(f) in Figs. 12, slopes of major fold lines $\psi=\pi/6$ have been chosen. However as far

as the continuity of patterns is satisfied, the angle φ can be chosen arbitrarily.

5. Manufacturing of Foldable Cylinders

By manufacturing cylinders with prescribed patterns, their foldability is investigated. Folding tests of the devised cylinders given by Fig. 12(c) and (e) were performed from a fully extended heights (about 90% of those of their developments). Appearances of the folding process are shown in Fig. 14(a) - (c), and (d) - (f), respectively. It was verified that the cylinders are folded smoothly rotating at their tops; it is expected that the cylinders processed like Fig. 14 (a) and (d) will be folded as shown in these photos. It was confirmed by these experiments that loads required to fold are as small as 20 - 40 N (diameter of cyrindrical shell; about 100 mm).

6. Consideration of Foldable Cylinder

By choosing $N=6$, several models of foldable cylinders consisting of triangle or trapezoid elements were divised. N sided regular polygon type foldable cylinders are designed by taking $(N-2)/N\cdot\pi$ for inner angle of the polygon ($N>3$). By selecting folding angles and the length between fold lines adequately, and also deviding the folding angles as in Fig. 11 (a) and (b), it is also possible to design foldable cylinders of irregular polygon or star shaped cross sections.

When foldable cylinders are made of thin polymer sheet, it is not difficult to process them as in Fig. 14 (a) and (d). Then it is expected that foldable bottles and other containers can be manufactured without great difficulty.

Foldable cylindrical shells constituted by spiral fold lines have been superior in their extensibility to those of horizontal major fold lines. This fact is quite suggestive to improve foldable structures. The detailed discussion for the extensibility is left to succeeding reports. It is noted here that axial expansion/contraction of these models is produced in folding manner. Hence it is completely different from bellows-type systems which always induce large elastic deformation in their parts.

7. Summary

Folding methods of flat sheets as well as cylindrical shells were discussed by using origami models. The obtained results are summarized as follows.

(1) New folding patterns of flat sheets and circular membranes are presented.

(2) New models of foldable cylinders, whose developments consist of scalene triangles or spiral configurations, were devised.

(3) By using newly prescribed patterns and using polymer sheets, all models were manufactured and their foldablility were studied. The models have been perfectly folded, and it has been confirmed that manufacturing of foldable goods becomes possible.

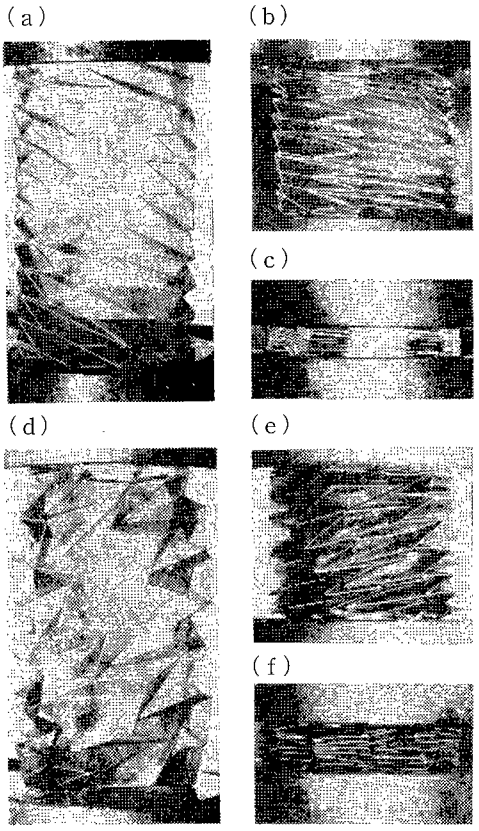

Fig. 14 Folding processes of polypropylene thin (0.2 mm) circular tubes (models shown in Fig. 12(c) and (e))

References

(1) Natori, M., Membrane Structures in Space, Trans. Jpn. Soc. Mech. Eng., (in Japanese), Vol. 102, No. 962 (1999), pp. 48-50.

(2) Miura, K. and Natori, M., 2-D Array Experiment on Board a Space Structure, Space Solar Power Rev., Vol. 5 (1985), pp. 346-356.

(3) Miura, K., Concepts of Deployable Space Structures, Int. J. of Space Structure, Vol. 8 (1993), pp. 3-16.

(4) Kobayashi, H., Kresling, B. and Vincent, J.F.V., The Geometry of Unfolding Tree Leaves, Proc. R. Soc. Lond. B 265 (1998), pp. 147-154.

(5) Fushimi, K., Origami no Kagaku, Science (Japan), Oct. Supplement (1980).

(6) Guest, S.D. and Pellegrino, S., The Folding of Triangulated Cylinders, Part I; Geometric Considerations, J. of Appl. Mech., Vol. 61 (1994), pp. 773-777.